Journal of Pharmaceutical Sciences 109 (2020) 353-363

Contents lists available at ScienceDirect

Journal of Pharmaceutical Sciences

journal homepage: www.jpharmsci.org

Pharmaceutical Biotechnology

Characterization of Excipient Effects on Reversible Self-Association, Backbone Flexibility, and Solution Properties of an IgG1 Monoclonal Antibody at High Concentrations: Part 2

Yue Hu [1, 2], Ronald T. Toth IV [1, 2], Sangeeta B. Joshi [1, 2], Reza Esfandiary [3], C. Russell Middaugh [1, 2], David B. Volkin [1, 2, *], David D. Weis [1, 4, *]

[1] Department of Pharmaceutical Chemistry, University of Kansas, Lawrence, Kansas 66047
[2] Macromolecule and Vaccine Stabilization Center, University of Kansas, Lawrence, Kansas 66047
[3] Department of Formulation Sciences, MedImmune LLC, Gaithersburg, Maryland 20878
[4] Department of Chemistry and R.N. Adams Institute of Bioanalytical Chemistry, University of Kansas, Lawrence, Kansas 66045

ARTICLE INFO

Article history:
Received 29 March 2019
Revised 13 May 2019
Accepted 4 June 2019
Available online 11 June 2019

Keywords:
monoclonal antibody
protein-protein interactions
reversible self-association
phase separation
excipient effects
hydrogen exchange-mass spectrometry
colloidal stability
local dynamics

ABSTRACT

In this work, we continue to examine excipient effects on the reversible self-association (RSA) of 2 different IgG1 monoclonal antibodies (mAb-J and mAb-C). We characterize the RSA behavior of mAb-C which, similar to mAb-J (see Part 1), undergoes concentration-dependent RSA, but by a different molecular mechanism. Five additives that affect protein hydrophobic interactions to varying extents including a chaotropic salt (guanidine hydrochloride), a hydrophobic salt (trimethylphenylammonium iodide), an aromatic amino acid derivative (tryptophan amide hydrochloride), a kosmotropic salt (sodium sulfate, Na_2SO_4), and a less polar solvent (ethanol) were evaluated to determine their effects on the solution properties, molecular properties, and RSA of mAb-C at various protein concentrations. Four of the 5 additives examined demonstrated favorable effects on the pharmaceutical properties of high concentration mAb-C solutions (i.e., lower viscosity and weakened protein-protein interactions, PPIs) with a ranking order of guanidine hydrochloride > trimethylphenylammonium iodide > tryptophan amide hydrochloride > ethanol as measured by various biophysical techniques. Conversely, addition of Na_2SO_4 resulted in less desirable solution properties and enhanced PPIs. The effect of these 5 additives on mAb-C backbone dynamics were evaluated by hydrogen exchange-mass spectrometry (at high vs. low protein concentrations) to better understand their effects on the molecular sites of RSA in mAb-C.

Introduction

Monoclonal antibodies (mAbs) are parenterally administered to patients as biotherapeutic drugs primarily by intravenous or subcutaneous injection.[1] The latter route offers the potential of reducing costs, saving time, and increasing patient compliance by having patients self-administer.[1-3] As outlined in detail in the Part 1 companion paper,[4] successful formulation of mAbs as high-concentration protein dosage forms is a challenge in terms of both protein instability (e.g., aggregation and reversible self-association [RSA]) and pharmaceutical solution properties (e.g., high viscosity).

One of the challenges of formulating mAbs at high concentrations is caused by RSA, a phenomenon in which native proteins undergo specific, noncovalent, concentration- and temperature-dependent, reversible protein-protein interactions (PPIs).[1,5-12] Formation of intermolecular protein complexes by RSA can dramatically increase

Abbreviations used: BB, base buffer; CDR, complementarity-determining regions; CG-MALS, composition-gradient multiangle light scattering; C_H1-C_H3/C_L, constant domains of the heavy/light chain; DLS, dynamic light scattering; Fab, antigen-binding fragment; Fc, crystallizable fragment; GdnHCl, guanidine hydrochloride; HX-MS, hydrogen exchange-mass spectrometry; LC, light chain; mAbs, monoclonal antibodies; PPIs, protein-protein interactions; RSA, reversible self-association; TMPAI, trimethylphenylammonium iodide; TrpNH2HCl, tryptophan amide hydrochloride.

Current address for Dr. Hu: Bristol-Myers Squibb, 1 Squibb Dr., New Brunswick, New Jersey, 08901.

Current address for Dr. Toth: GSK Vaccines, 14200 Shady Grove Road, Rockville, Maryland, 20850.

This article contains supplementary material available from the authors by request or via the Internet at https://doi.org/10.1016/j.xphs.2019.06.001.

* *Correspondence to:* David D. Weis (Telephone: +1-785-864-1377) and David B. Volkin (Telephone: +1-785-864-6262).

E-mail addresses: volkin@ku.edu (D.B. Volkin), dweis@ku.edu (D.D. Weis).

https://doi.org/10.1016/j.xphs.2019.06.001
0022-3549/

solution viscosity, resulting in pharmaceutical development challenges including high pressure during processing (e.g., sterile filtration) and clinical administration (injection via syringe).[13] In addition, aggregation nuclei might form, potentially leading to the formation of aggregates of varying sizes (i.e., small soluble aggregates, subvisible particles, and larger visible particulates). Such aggregates might not only reduce antibody therapeutic potency but also could potentially generate unwanted immune responses.[14,15] Moreover, high opalescence and even phase separation can occur in high concentration mAb solutions.[6,7] For patients, injecting highly viscous or turbid mAb solutions should be avoided because of potential pain on injection and an inability to view the solution for the presence of particulates.[2] Based on these considerations, various strategies to mitigate RSA in high concentration mAb solutions are often required.

The 2 major approaches taken to reduce RSA in mAb candidates during their development are point mutations through protein engineering[16-18] and formulation development including the addition of excipients.[19,20] Both strategies are mAb specific and require systematic work for each individual mAb. For example, protein engineering approaches require site-specific information in the regions that initiate mAb-mAb interactions. Although point mutations can work well to reduce RSA, the binding affinity between the mAb and its antigen can also be potentially altered (i.e., increased or decreased), and the physicochemical stability profile of the mAb can also be affected. In addition, it is usually too late for a mAb molecule to be re-engineered once it enters clinical development as it will likely be considered a new molecular entity. Alternatively, formulation approaches focus on optimizing the environment around mAb molecules, rather than altering the mAb molecule itself. Although additives can be identified that reduce RSA, their effect(s) on mAb stability (i.e., conformational, colloidal, and chemical degradation pathways) and relative solubility in solution must be evaluated.

The companion paper in this issue describes an IgG1 mAb referred to as mAb-J, in which electrostatic interactions are the dominant force that drives RSA. This work (part 2) examines the effect of a series of additives on the RSA of a different human monoclonal IgG1 (mAb-C) that has been previously shown to undergo RSA by an apolar mechanism. As reported previously, high solution viscosity was observed for mAb-C at relatively high protein concentrations, and potential PPI sites on mAb-C as well as potential dominant interaction forces were identified,[21,22] as being increasingly driven by specific hydrophobic interactions as the solution pH increased from 6 to 8 (approaching the mAb-C isoelectric point [pI] range of 9.1–9.4).[21] Using hydrogen exchange-mass spectrometry (HX-MS) differential analysis of high versus low concentrations of mAb-C at pH 7.0, it was demonstrated that Fab-Fab interactions, including specific complementarity-determining regions (CDRs), rich in hydrophobic and aromatic amino acid residues, play a crucial role in the RSA of mAb-C.[21]

It has also been demonstrated that point mutation of specific hydrophobic amino acid residues in the mAb-C RSA regions manifested improved solution properties (reduced extent of PPIs).[16] Concomitantly, however, antigen-binding affinity of mAb-C decreased significantly (by ~200- to 400-fold).[16] Therefore, modulating mAb-C RSA by employing different additives (i.e., evaluating and better understanding the effect of these additives) at high protein concentrations was the major goal of this work. We, therefore, evaluated both solution and molecular behavior as well as backbone flexibility alterations of mAb-C at various protein concentrations in the absence and presence of 5 additives known to affect protein hydrophobic interactions to varying extents.

Based on a previous work showing that certain regions within specific CDRs in mAb-C (containing many hydrophobic and aromatic amino acid residues) were the dominant sites of interaction for mAb-C RSA,[21] we selected a series of additives to compare their RSA-disrupting properties including a chaotropic salt (guanidine hydrochloride [GdnHCl]), a hydrophobic salt (trimethylphenylammonium iodide [TMPAI]), an aromatic amino acid derivative (tryptophan amide hydrochloride [$TrpNH_2HCl$]), a kosmotropic salt (sodium sulfate [Na_2SO_4]), and a less polar solvent (ethanol). A variety of biophysical techniques were used to examine mAb-C solution properties as well as protein molecular behavior in the presence of the excipients. HX-MS was also used to better understand the effect of these additives on particular regions of mAb-C known to be involved in the RSA of mAb-C.

Materials and Methods

Materials

MedImmune LLC (Gaithersburg, MD) provided a highly purified IgG1 antibody (mAb-C) in a stock solution at 10 mg/mL. A base buffer (BB) solution, selected as the baseline condition to examine mAb-C RSA, contained 40 mM of potassium phosphate at pH 7.5. The stock solution of mAb-C was first concentrated to 70 mg/mL and then buffer exchanged into the desired BB solution (with and without various additives). Dialysis was performed using 3.5 kDa molecular weight cutoff membranes (Slide-A-Lyzer; Thermo Scientific, Rockford, IL) at 4°C and kept overnight against BB or BB with various additives (including 0.5 M GdnHCl; 150 mM Na_2SO_4; 150 mM TMPAI; 150 mM $TrpNH_2HCl$, 150 mM $PheNH_2HCl$, and 15% ethanol). Different excipient concentrations were used based on their relative hydrophobicity. For example, TMPAI, $TrpNH_2HCl$, $PheNH_2HCl$, and Na_2SO_4 were examined at a concentration of 150 mM due to these molecules possessing aromatic groups or displaying salting-out effects at higher concentrations. Because of the lack of these properties, elevated amounts of GdnHCl were used (0.5 M). Finally, as a cosolvent, 15% v/v ethanol was used, and even at this concentration, protein precipitation was noted in some experiments (see Results section). These additives were obtained from Sigma-Aldrich (St. Louis, MO) or ChemImpex International ("CII") (Wood Dale, IL).

Methods

The methods, including solution dynamic viscosity, dynamic light scattering, relative apparent solubility (thermodynamic activity) by a polyethylene glycol (PEG) precipitation method, composition-gradient multi-angle light scattering (CG-MALS), deuteration of excipients, HX-MS, and postlyophilization characterization of mAb samples using UV-visible spectroscopy, circular dichroism, and size exclusion chromatography (SEC), used in this study have been reported previously and are also presented in the Supplemental Methods section.[3,21,23,24] Additional methods that were used in this study are also described in the Supplemental Methods section including measurements of protein interaction parameters (k_{D2}) by dynamic light scattering (DLS), Karl-Fisher titration for moisture content analysis, and both bicinchoninic acid assay and SEC analysis for determination of protein concentration.

Homology Modeling and Protein-Additive Docking

A mAb-C homology model, built previously to demonstrate potential RSA regions at high protein concentrations,[25] was based on the mAb-C primary sequence, and crystal structures of an isolated crystallizable fragment (Fc) and an *in silico*–generated KOL/Padlan structure of an Fab.[26,27] The homology model was then prepared, charged, and minimized via a Molecular Operating Environment (MOE 2016 of Chemical Computing Group ULC).[28] The

CDRs of mAb-C were identified by MOE software based on sequence analysis of the variable regions. Hydrophobic patches of 170 Å^2 of solvent-accessible surface area were also identified in MOE. Simple local rigid body docking between mAb-C RSA interfaces and selected excipients was modeled using MOE software based on a combination of energetics and shape complementarity. Docking to model the excipients-mAb interface used 100 runs for each compound and a triangle marcher technique for placement stage, affinity dG for rescoring, and forcefield method for refining. Potential docking locations and lowest energy poses (less than −7 kcal/mol) were demonstrated using a mAb-C homology model.

Results

Additive Effects on mAb-C Solution Properties

The viscosity of mAb-C solutions of increasing protein concentration was measured in BB alone and in the presence of 5 additives at 2 temperatures, 4°C and 25°C. As shown in Figure 1, the dynamic viscosity values increased exponentially as a function of protein concentration. For example, values of 12.8 and 3.5 centipoise (cP) are seen at a protein concentration of 60 mg/mL in BB alone at 4°C and 25°C, respectively. The addition of the different additives to mAb-C solutions perturbed the solution dynamic viscosity at all temperatures. GdnHCl had the largest effect on reducing the viscosity of mAb-C solutions, showing values of 4.7 and 2.1 cP at a protein concentration of 60 mg/mL at 4°C and 25°C, respectively. Similarly, both TMPAI and $TrpNH_2HCl$ also decreased the solution viscosity of mAb-C with TMPAI showing comparatively greater effect. Because solution viscosity is related to PPIs, especially at high mAb-C concentrations, the ability of these 3 excipients to reduce viscosity is probably because of their RSA-disrupting properties.[2,8,20] Interestingly, Na_2SO_4 had the opposite effect, resulting in increased mAb-C solution viscosity. For example, at a protein concentration of 60 mg/mL, a viscosity value of 16.5 cP was observed at 4°C in BB containing Na_2SO_4 compared to 12.8 cP in BB alone. Owing to varying amounts of precipitation observed with some of the mAb-C solutions at 4°C, dynamic viscosity measurements for mAb-C were not performed in 15% (v/v) ethanol.

Additive Effects on the Physical Properties of mAb-C

The relative apparent solubility (thermodynamic activity) as determined by $PEG_{10,000}$ induced precipitation assay is not only an indicator of PPIs[29] but also provides a practical rank ordering of excipient effects on relative protein solubility. Sigmoidal curves of mAb-C protein concentration as a function of the amount of % $PEG_{10,000}$ were obtained in the absence and presence of additives as shown in Figure 2a. The $\%PEG_{midpt}$ values (the amount of $PEG_{10,000}$ needed to precipitate half of the total protein in solution) obtained for mAb-C in the presence of each additive are shown in Figure 2b. In BB alone, a $\%PEG_{midpt}$ value of 4.0% was obtained, while in the presence of the additives, this value changed in different directions and varying magnitudes. For example, GdnHCl, TMPAI, and $TrpNH_2HCl$ showed increased $\%PEG_{midpt}$ values of 7.4%, 5.8%, and 5.3%, respectively, indicating higher relative solubility of mAb-C in comparison to that in BB. With ethanol, however, the relative solubility of mAb-C decreased showing a $\%PEG_{midpt}$ value of 2.0%. Moreover, in the presence of Na_2SO_4, mAb-C showed higher relative solubility ($\%PEG_{midpt}$ value of 5.0%) at an excipient concentration of 150 mM but lower relative solubility ($\%PEG_{midpt}$ value of 2.5%) in 0.5 M Na_2SO_4. Finally, the apparent solubility values in the absence of $PEG_{10,000}$ in solution were estimated by extrapolation of the linear portion of data in Figure 2a as plotted in Figure 2c and displayed in Figure 2d. The results are overall consistent with the trend of excipient effects on the relative solubility of mAb-C as reflected by the $\%PEG_{midpt}$ values.

The effect of these 5 additives on the average size of mAb-C complexes in solution were determined by DLS as shown in Figure 3. In general, the hydrodynamic diameter of an antibody molecule is around 9-12 nm.[30] In contrast, DLS measurements showed a hydrodynamic diameter of 22 nm for mAb-C in the BB at 10 mg/mL, indicating mAb-C molecules are prone to form larger size complexes. In the presence of GdnHCl, mAb-C showed a diameter value of 12 nm (consistent with monomer), indicating a disruption of the complexes. Similarly, TMPAI, $TrpNH_2HCl$, and ethanol also possessed some ability to reduce mAb-C hydrodynamic diameter by disrupting PPIs, displaying values of approximately 13 nm, 15 nm, and 18 nm, respectively. The addition of Na_2SO_4 resulted in the opposite effect, increasing the hydrodynamic diameter of mAb-C to 31 nm, a result consistent with Na_2SO_4 effects on mAb-C solution viscosity (indicating an ability to promote intermolecular interactions among mAb-C molecules). Dispersity values between ~10% and 20% were observed for all the samples.

The protein interaction parameter, $k_{D2,}$ for mAb-C was also measured by DLS in the presence and absence of the 5 additives. Positive and negative values for k_{D2} indicate repulsive and attractive interactions between mAb-C molecules, respectively. As shown

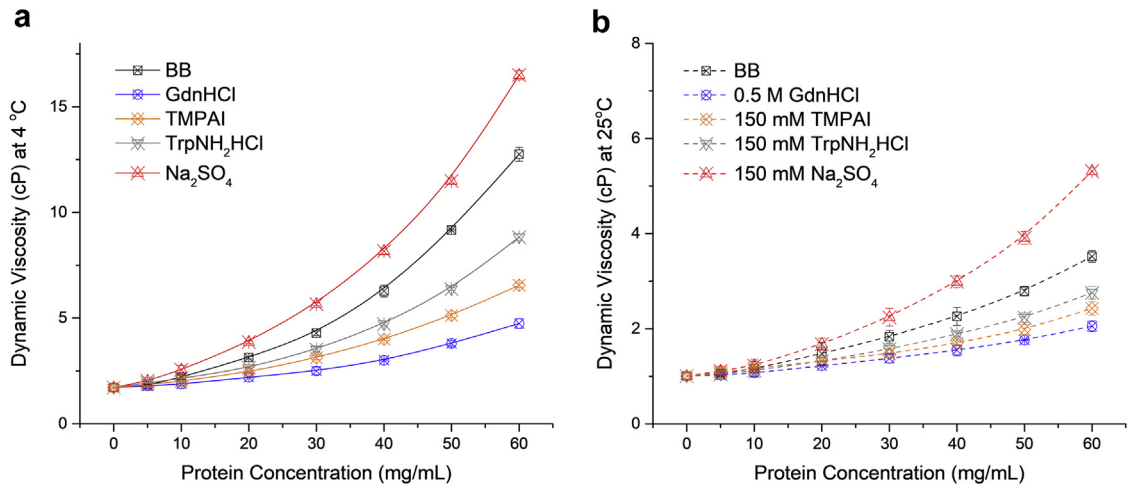

Figure 1. Effect of additives on the dynamic viscosity of mAb-C solutions at varying protein concentrations at (a) 4°C and (b) 25°C. Excipients were at 150 mM, except GdnHCl (0.5 M) and ethanol (15% v/v) in base buffer (BB). Data are presented as mean ± standard deviation; $n = 3$.

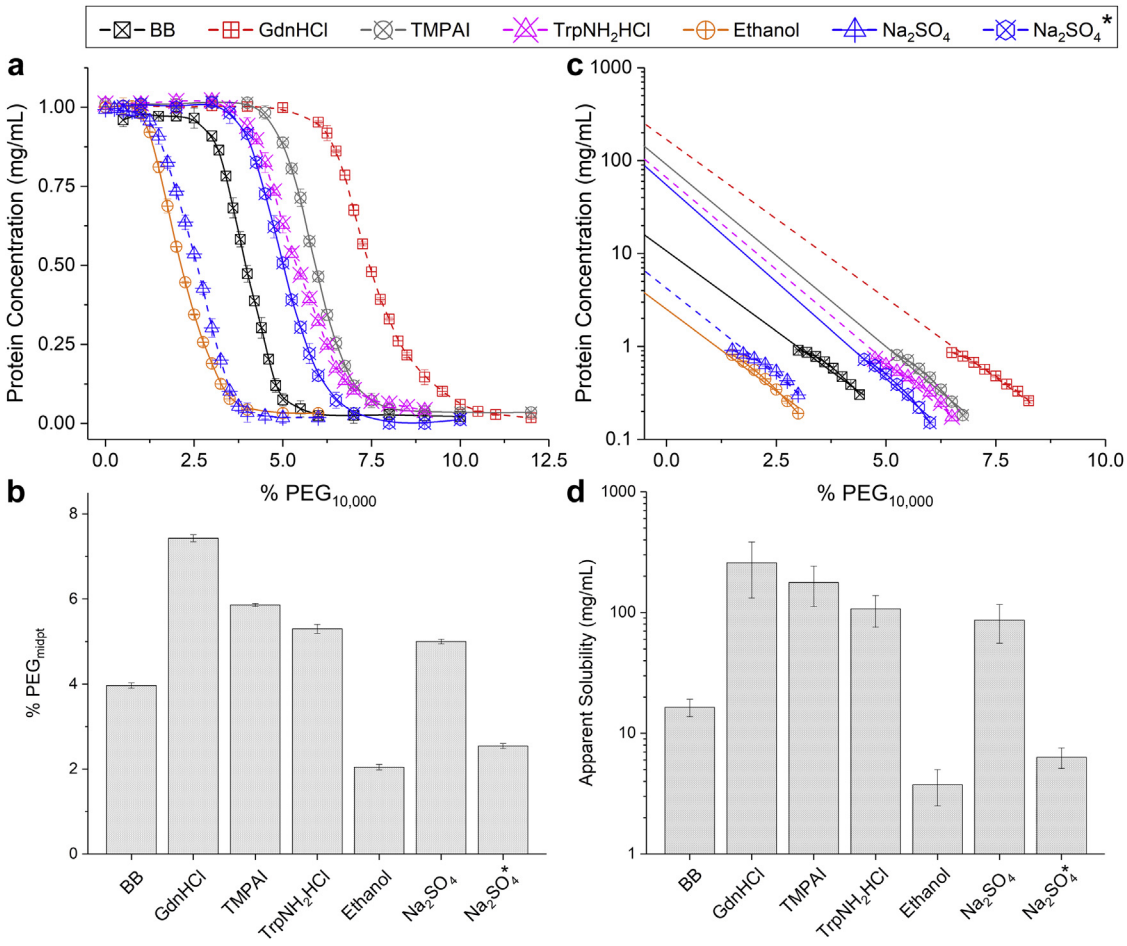

Figure 2. Relative apparent solubility (thermodynamic activity) of mAb-C in the presence of different additives as measured by $PEG_{10,000}$ induced precipitation. (a) Change of mAb-C concentration as a function of $\%PEG_{10,000}$ added to solution (data fit by sigmoidal curves). (b) $\%PEG_{midpt}$ values are shown in a bar chart, indicating the amount of $PEG_{10,000}$ that was needed to precipitate half of the total protein from the solution. (c) Apparent solubility values were obtained from *y*-axis extrapolation of data points in the transition range shown in panel (a and d) Comparison of the apparent solubility values obtained for mAb-C in the absence and presence of various additives. Two concentrations of sodium sulfate (150 mM for "Na_2SO_4" and 0.5 M for "Na_2SO_4*") were used for this study. Other excipient solutions had a concentration of 150 mM, except GdnHCl (0.5 M) and ethanol (15% v/v) in BB. Multiple methods were employed to determine protein concentration, including A_{280nm} for mAb-C in BB, and BB in the presence of GdnHCl, ethanol, and Na_2SO_4; bicinchoninic acid assay for mAb-C solution in the presence of TMPAI (Supplemental Fig. S1a), and SEC method for mAb-C solution in the presence of $TrpNH_2HCl$ (Supplemental Fig. S1b). Data are presented as mean ± standard deviation; $n = 3$.

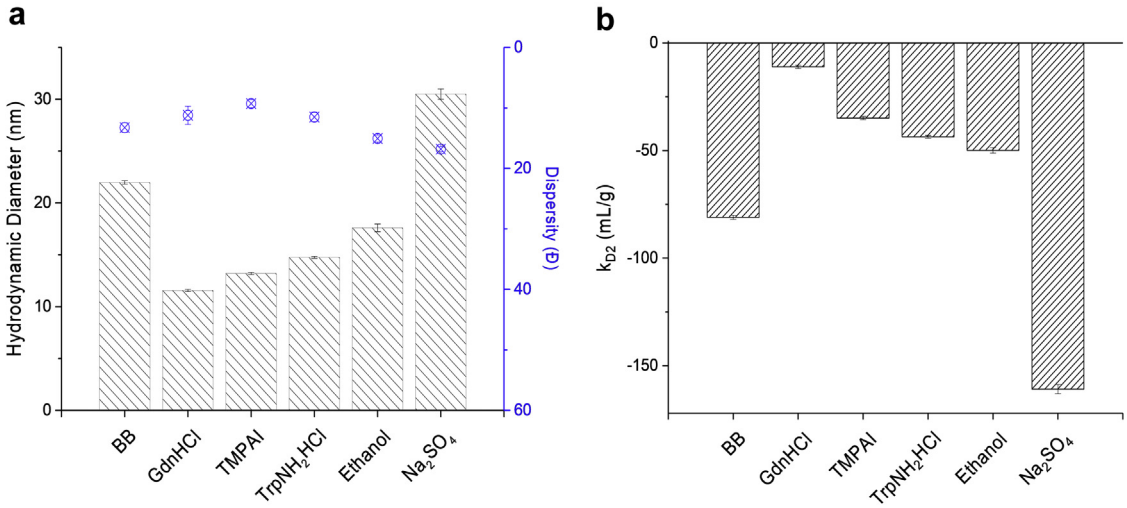

Figure 3. Effect of additives on mAb-C hydrodynamic diameter and protein interaction parameter (k_{D2}) as determined by dynamic light scattering. (a) Hydrodynamic diameter (bars, left axis) and dispersity values (squares, right axis) were determined at a protein concentration of 10 mg/mL, and (b) k_{D2} values were calculated from a series of mAb-C hydrodynamic diameter measurements from 1 to 10 mg/mL protein concentrations at 25°C. Concentration of additives was 150 mM, except GdnHCl (0.5 M) and ethanol (15% v/v) in BB. DLS cumulative data were weighted by intensity. Data are presented as mean ± standard deviation; $n = 3$.

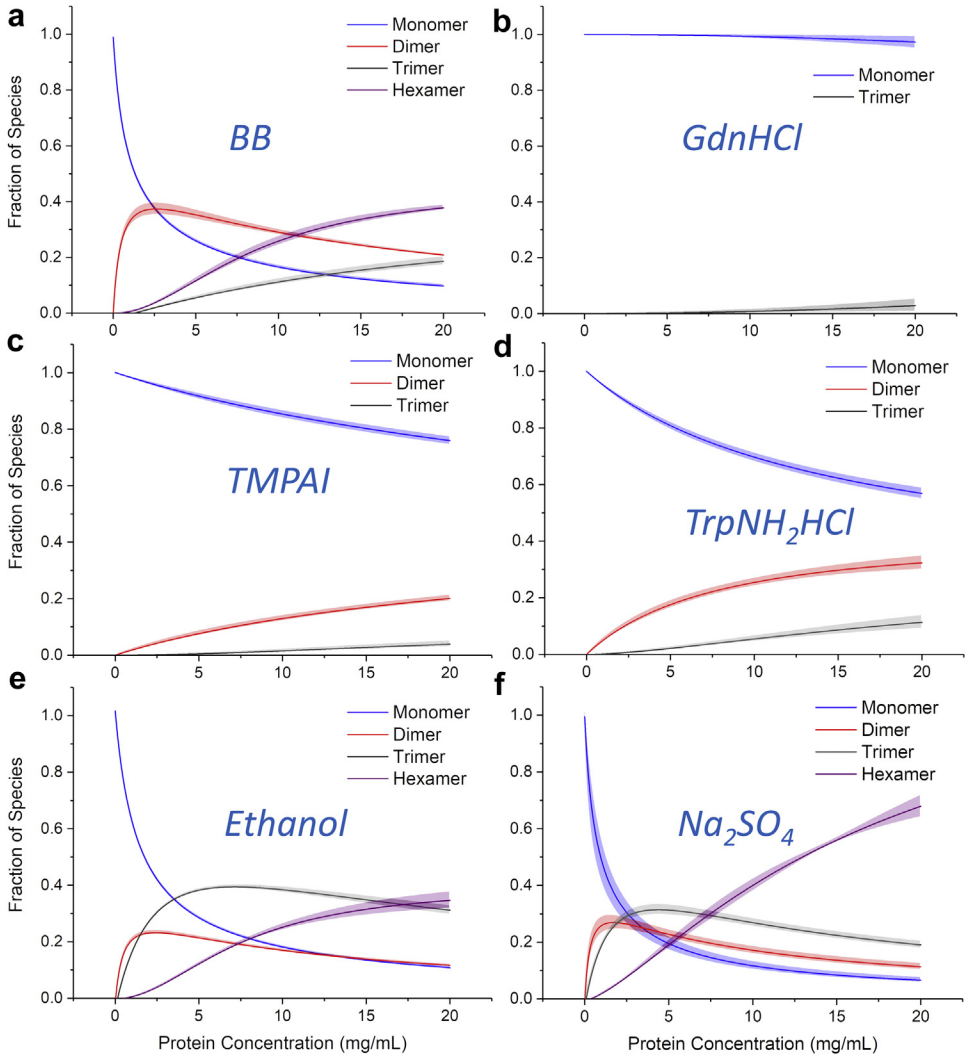

Figure 4. Effect of additives on the self-association induced complexes of mAb-C as determined by static light scattering from CG-MALS analysis. The fraction of various species was determined as a function of protein concentration in the absence and presence of different additives in base buffer (BB) containing (a) BB alone, or BB with (b) GdnHCl, (c) TMPAI, (d) $TrpNH_2HCl$, (e) ethanol, and (f) Na_2SO_4. The concentration of the excipients was 150 mM, except GdnHCl (0.5 M) and ethanol (15% v/v). Measurements were performed at room temperature. All data are presented as mean ± standard deviation; $n = 3$.

in Figure 3b, a k_{D2} value of −81 mL/g was measured for mAb-C in BB, indicating extensive attractive interactions between mAb-C molecules. Values of k_{D2} of −11, −35, −44, or −50 mL/g in the presence of GdnHCl, TMPAI, $TrpNH_2HCl$, or ethanol, respectively, were observed indicating their ability to weaken mAb-C PPIs. Na_2SO_4 resulted in a k_{D2} value of −161 mL/g consistent with stronger attractive interactions for mAb-C. In summary, the values of both hydrodynamic diameter and protein interaction parameter (k_{D2}) as measured by DLS showed similar trends of excipient effects on RSA of mAb-C.

The size and nature of mAb-C complexes in solution were further examined by static light scattering using CG-MALS as shown in Figure 4. The fraction of each species was calculated based on curve-fitted scattering signal as a function of protein concentration. For example, as shown in Figure 4a, the monomeric fraction of mAb-C in the BB decreased as the protein concentration increased. Concomitantly, multimers of mAb-C including dimer, trimer, and hexamer increased. In the presence of 0.5 M GdnHCl, the distribution of species versus protein concentration was dramatically altered. As shown in Figure 4b, >95% of mAb-C remained monomeric across the concentration range examined. In Figures 4c and 4d, it can be seen that the addition of 0.15M TMPAI and $TrpNH_2HCl$ reduced the extent of complex formation for mAb-C, but to a lesser extent than GdnHCl, protecting monomeric mAb-C from becoming oligomeric species. In contrast, mAb-C in a 15% ethanol-containing solution showed a similar speciation profile, but comparatively different multimer pattern, compared to BB alone (Fig. 4e). Finally, as shown in Figure 4f, a rapid decrease of monomeric mAb-C along with a rapid increase of hexamers were observed in mAb-C solution in the presence of 0.15M Na_2SO_4 as the mAb-C concentration was increased.

To better compare and visualize these additive effects on mAb-C solution and molecular properties, the preceding results can be displayed as radar charts (Fig. 5). Comparative results for dynamic viscosity values (at a protein concentration of 60 mg/mL at 4°C), apparent solubility values, fraction of monomeric mAb-C from CG-MALS (at 20 mg/mL), and protein interaction k_{D2} values are displayed in Figures 5a-5d, respectively. Each corner of the individual radar chart represents a solution condition (BB, BB with GdnHCl, TMPAI, $TrpNH_2HCl$, ethanol, and Na_2SO_4 clockwise from the top corner). By summarizing the data together, differential effects of the 5 different additives on mAb-C can be more easily assessed.

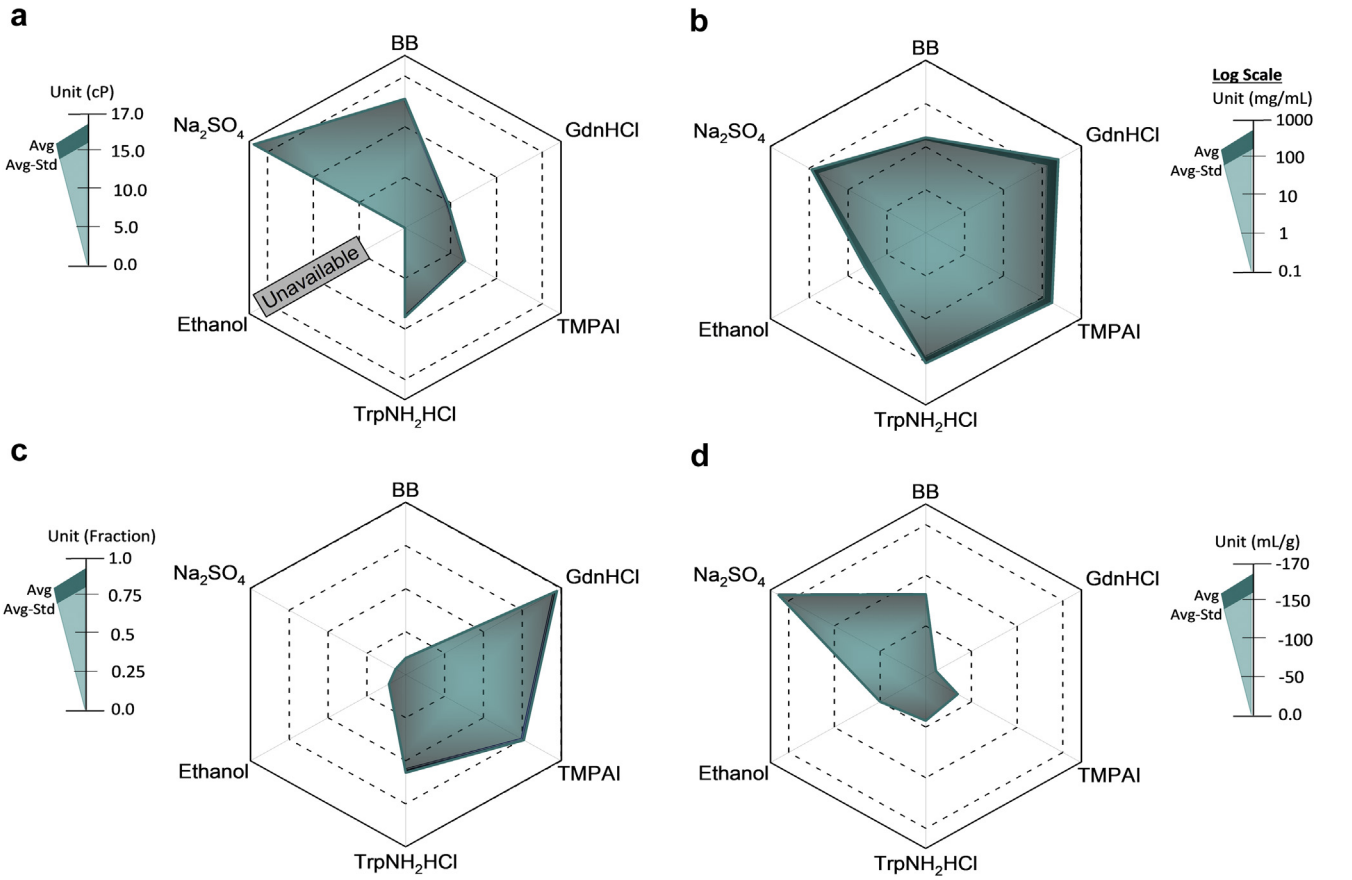

Figure 5. Radar chart array analysis to better visualize additive effects on mAb-C solution and molecular properties. Except for GdnHCl (0.5 M) and ethanol (15% v/v), all other additive solutions have a concentration of 150 mM. Specifically, (a) dynamic viscosity values at protein concentration of 60 mg/mL, (b) mAb-C apparent solubility values in log scale, (c) the fraction of mAb-C monomer at the concentration of 20 mg/mL as measured by CG-MALS, and (d) the values of the protein interaction parameter (k_{D2}). The distance between the perimeters of the 2 polygons (along an axis) is 1 standard deviation. Triplicate measurements were performed.

Three additives show consistent RSA-disruption effects with a ranking order of GdnHCl > TMPAI > $TrpNH_2HCl$. In contrast, although ethanol demonstrates an ability to disrupt PPIs of mAb-C, it had detrimental effects on relative solubility. Finally, Na_2SO_4 consistently shows RSA promotion effects on mAb-C across the different measurements at high concentrations.

Alteration of mAb-C RSA Propensity by Additives as Measured by HX-MS

To better understand backbone flexibility alterations of mAb-C in the presence of these 5 additives at high versus low protein concentrations, HX-MS was used. The deuterium environment of mAb-C was provided by a lyophilization-reconstitution method at 5 and 60 mg/mL, as described previously.[21] Briefly, mAb-C was first lyophilized and then reconstituted with excipient-containing D_2O. To confirm the integrity of lyophilized mAb-C samples, analytical characterization of reconstituted mAb-C was performed, as shown in Supplemental Figure S2 and Supplemental Table S1. As shown by a combination of visual inspection (acceptable cake integrity), moisture content (0.5%-2.0% water by Karl Fischer titration), overall secondary structure (similar CD spectra), and absence of aggregation (~99% protein recovery with 98%-99% monomer as determined by UV spectroscopy and SEC analysis, respectively), lyophilized mAb-C samples retained their integrity after lyophilization and reconstitution. Thus, these samples are suitable for use in HX-MS analysis.

After reconstitution with D_2O buffer to trigger mAb-C amide-hydrogen labeling in the presence or absence of the 5 additives, a 3600 s incubation was carried out based on the time course of HX exchange for mAb-C as determined from a previous study in our laboratories.[21] The reaction was then quenched, the mAb was digested with immobilized pepsin, and the uptake of deuterium in each peptide was determined by liquid chromatography-MS as described in the Supporting Information. Peptides were obtained by immobilized pepsin digestion and analyzed by liquid chromatography-MS as described in the Supporting Information. A total of 200 peptides were identified (see Supplemental Table S2), providing 98% and 100% sequence coverage of the heavy chain and light chain (LC), respectively. The mass difference for each peptide was obtained based on 5 and 60 mg/mL protein concentrations, both with and without excipients. A value of 0.67 Da, representing a 99% confidence interval significance criterion for peptide mass differences was used to identify significantly different HX between 60 and 5 mg/mL. As shown in Figure 6, HX differences for each peptide are plotted in the absence and presence of excipients. For panel a, ΔHX = HX (BB, 60 mg/mL) − HX (BB, 5 mg/mL); and for panels b-f: ΔHX = HX (BB + excipient, 60 mg/mL) − HX (BB + excipient, 5 mg/mL).

Although RSA sites were determined previously for mAb-C at 60 mg/mL at pH 7.0,[21] additional regions of mAb-C might be involved in PPIs at pH 7.5, used here to deliberately increase mAb-C RSA propensity. Five significantly protected regions of mAb-C at pH 7.5 were observed, as shown in Figure 6a. As reported previously, the

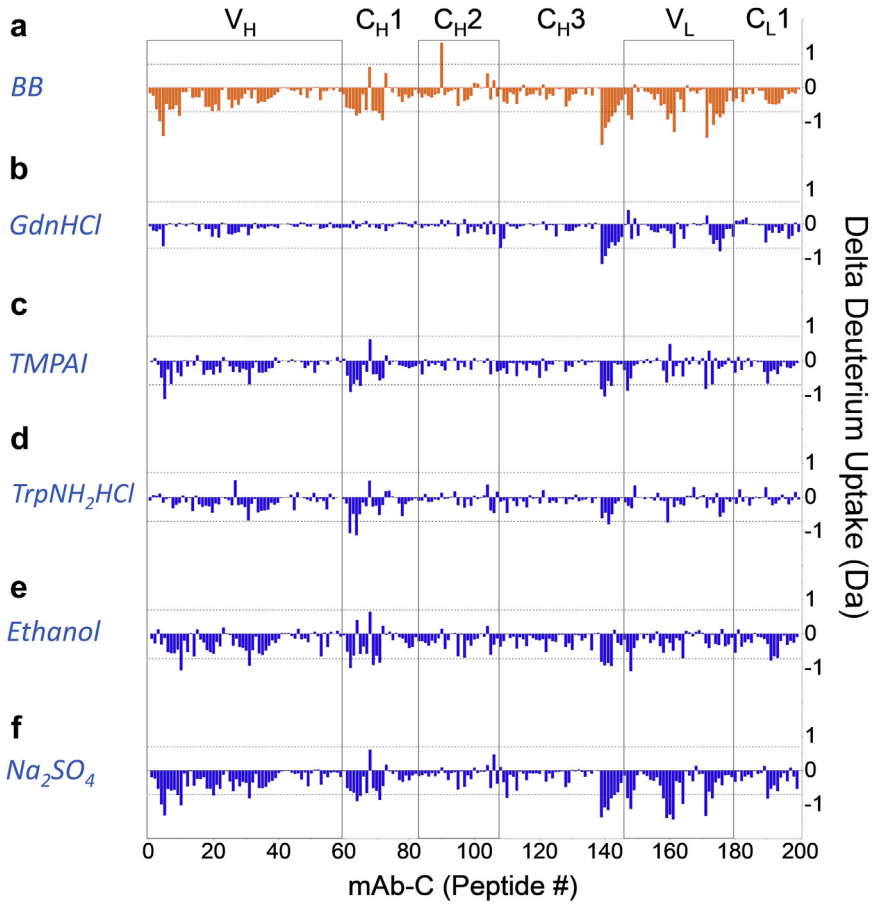

Figure 6. Effect of additives on mAb-C RSA and backbone flexibility by mass difference plot from HX-MS. (a) Mass difference of each peptide between 60 mg/mL and 5 mg/mL of mAb-C in BB. Panels (b) GdnHCl (0.5 M), (c) TMPAI (150 mM), (d) $TrpNH_2HCl$ (150 mM), (e) ethanol (15% v/v), and (f) Na_2SO_4 (150 mM) show effects of different excipients on alteration of protein interactions and on local peptide flexibility. Alternate backgrounds indicate antibody domain boundaries. Positive ΔHX values imply increased backbone flexibility, whereas negative values indicate the opposite. The dashed horizontal lines are the 99% confidence criteria. Three independent HX measurements were performed. The peptides are numbered in order from the N-to-C termini of the heavy chain followed by the light chain of mAb-C. See Supplemental Table S2 for amino acid residue numbers of mAb-C that correspond to each peptide number.

CDR L2 region was the primary RSA site for mAb-C at pH 7.0, where it showed strong protection at high protein concentration.[21] The CDR H2 was also observed to have increased protection at high protein concentrations, especially at shorter labeling times.[21] In this study (Fig. 6a), consistent with these previous results, significant protection was observed covering the CDR L2 region (sequence L_{47}LIYVASSLQSGVPSRFSGSGSGT$_{70}$, peptide 156-163); however, HX differences in the CDR H2 region did not exceed the significance limit at the single HX time point examined. Additional regions of mAb-C showed protection at pH 7.5 covering CDR H1 (sequence Q_1VQLVQSGAEVKKPGASVKVSCYTFTGYYMHW$_{32}$, peptide 3-11), the beginning region of C_H1 (sequence V_{121}TVSSASTKGPSVF-PLAPSSKSTSGGTAALGCLVKDY FPEPVTVSWNSGALTSGVHTFPAVL$_{182}$, peptide 61-70), and the end region of C_H3 (sequence S_{432}CSVMHEALHNHYTQKSLSLSPG$_{454}$, peptide 139-145), and CDR L3 (sequence A_{84}TYYCQQANSFPWTFGQGTKVEIKRTVAAPSVF$_{116}$, peptide 171-178), indicating extensive, multiregion intermolecular interactions.

Different additives were examined for their ability to either promote or disrupt regions of RSA within mAb-C. Consistent with the biophysical results, the most efficient solute in terms of disrupting RSA interaction sites within mAb-C was GdnHCl (Fig. 6b), in which essentially all the RSA sites were diminished except for the 1 located in the C_H3 region. As shown in Figures 6c and 6d, TMPAI and $TrpNH_2HCl$ also had the ability to disrupt RSA between mAb-C molecules, especially in the CDR H1, CDR H2, CDR L2, and CDR L3 regions, although some weak protection still exists. For other regions of RSA, however, these 2 additives did not affect mAb-C RSA-induced protection. As for ethanol effects (Fig. 6e), only the RSA regions on the LC variable regions of mAb-C were disrupted, and little effect was seen on the other RSA sites. In contrast, as shown in Figure 6f, Na_2SO_4 promoted protection during deuterium exchange of mAb-C, especially within the RSA regions.

To better visualize these specific RSA regions on mAb-C at pH 7.5, the HX-defined RSA interface is shown mapped onto a mAb-C homology model as shown in Figure 7. Molecular modeling using MOE software (see Methods section) was used to examine additive binding as shown in Figure 8. The colored structures highlight the CDRs, while the remaining regions of the mAb are shown in white. The RSA interaction sites, based on HX-MS results, are highlighted in the space-filling representation as shown on the left-side panel in Figure 7. This shows that the variable regions of both the heavy and light chains are primarily responsible for mAb-C RSA, with a small hydrophobic site at the end of C_H3 domain also contributing to RSA. As an additional analysis, hydrophobic patches, shown in green areas on the right-side panel homology model in Figure 7, were identified in the homology model. Interestingly, some of the top-ranked hydrophobic patches (greater than 200 $Å^2$ solvent-accessible surface area) overlap with the RSA sites. Modeling based on local rigid docking was then performed at the major RSA rites in the CDRs of both heavy and LCs of mAb-C with 3 of the additives, $GdnH^+$, $TMPA^+$, and $TrpNH_2H^+$. Interactions stronger

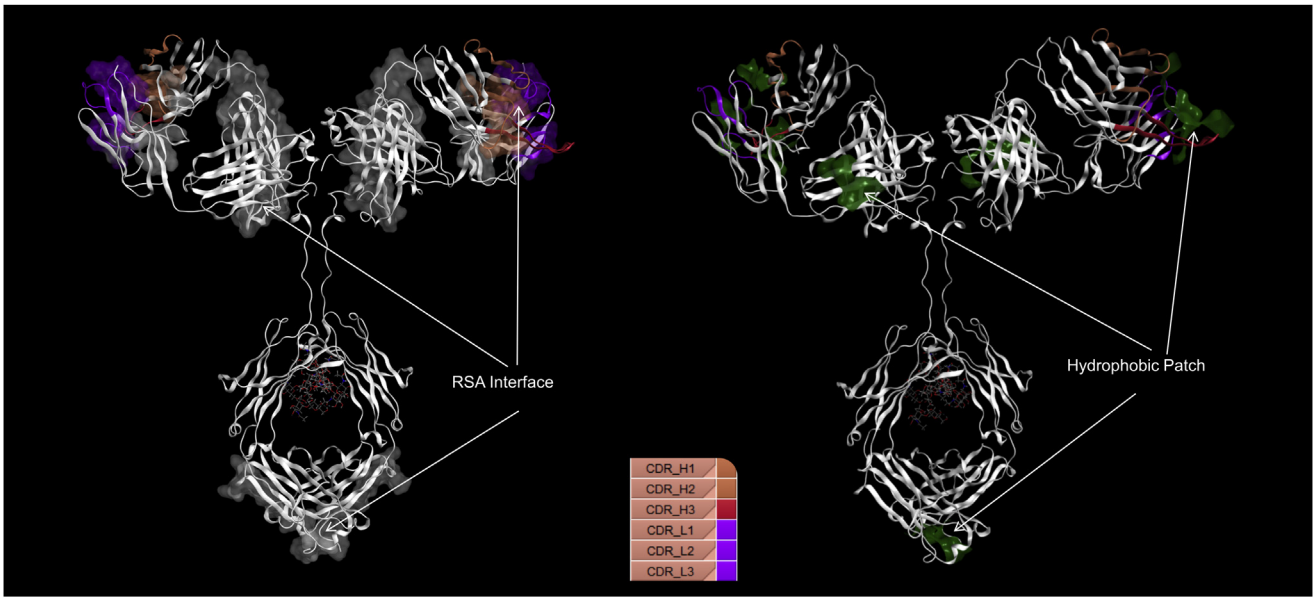

Figure 7. RSA interfaces defined and hydrophobic patches visualized on mAb-C. RSA interfaces of mAb-C, as defined by HX protection, are shown on the left in space-filling representation. Brown, red, and purple colors denote CDR H1, H2, H3, and CDR L1, L2, and L3, respectively. Hydrophobic patches (>200 Å^2, displayed in green) predicted by homology modeling using the Molecular Operating Environment (MOE) are shown on the right side.

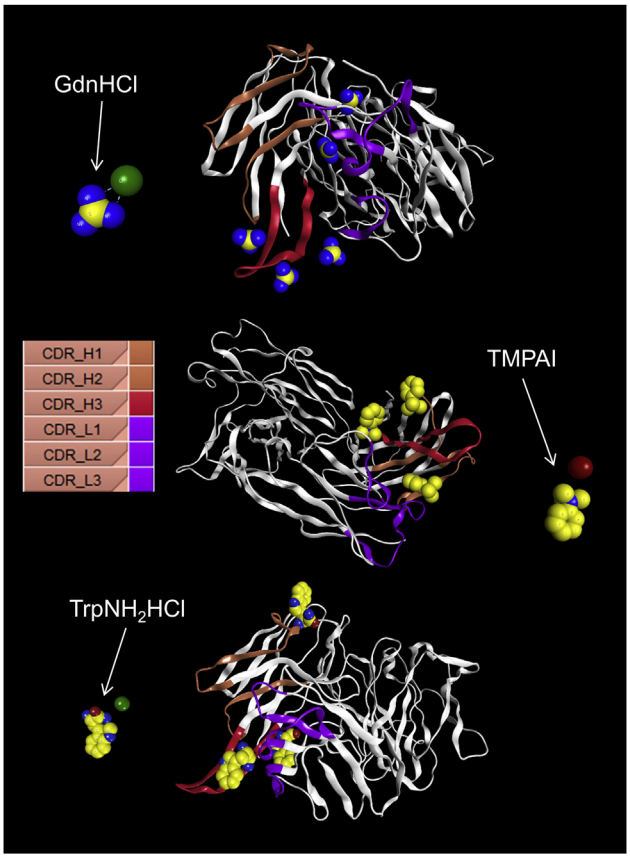

Figure 8. Local rigid docking of additives to identify favorable locations for binding on the Fab RSA sites of mAb-C at pH 7.5 calculated using MOE. Top-ranking candidates (below −7 kcal/mol) are shown on the Fab domain of the mAb-C homology model. For additive molecules, blue, yellow, red, green, and dark red represent nitrogen, carbon, oxygen, chloride, and iodide, respectively.

than −7 kcal/mol are shown on the Fab homology model of mAb-C in Figure 8. Five locations were found for $GdnH^+$ to interact with these mAb-C CDRs, while only 3 locations were detected for $TMPA^+$ and $TrpNH_2H^+$.

Discussion

Although protein engineering approaches have been shown in some cases to mitigate mAb intermolecular PPIs (and thus optimizing solution properties at high mAb concentrations),[16,17,31,32] a more straight-forward strategy (that does not alter the molecule itself) is excipient addition to improve the solution properties of mAbs at high concentrations. This can be pursued by either an excipient screening approach to semiempirically identify stabilizers[33] or by a more rational additive selection process based on a mechanistic understanding of RSA interactions for a particular mAb (as outlined in the companion paper in this issue with mAb-J).[4] In this work, we continue to examine the latter, more targeted approach to excipient selection by using HX-MS to identify regions of mAb-C (and associated molecular mechanisms), resulting in a more rational selection of additives to disrupt specific RSA interactions within a mAb.

As previously reported, a major RSA site on mAb-C was CDR L2 at pH 7.0. This involved regions containing hydrophobic and aromatic amino acid residues that appeared to result in PPIs among mAb-C molecules.[21] In this work, as we increased solution pH from 7.0 to 7.5, not only the CDR L2 region but also the additional regions within mAb-C showed protection from hydrogen exchange when comparing high versus low protein concentrations by HX-MS (Fig. 6). This indicates more PPI sites mediated RSA of mAb-C under these conditions. Because mAb-C has an isoelectric point (pI) ranging from 9.1 to 9.4 (data not shown), the protein will have less net positive charge, and thus weaker charge repulsion, presumably allowing mAb-C molecules to more easily self-associate at pH 7.5 (vs. pH 7.0). Computational mapping of hydrophobic patches on mAb-C, as shown in Figure 7, is in general agreement with the protected surfaces identified by HX-MS, consistent with apolar

interactions being a major force that drives mAb-C RSA. It is quite possible, however, that additional cross-interaction (e.g., Fab-Fab, Fab-Fc) sites between mAb-C molecules under these conditions (BB at pH 7.5) form, leading to additional interaction networks.[19,21,23,34,35] Hydrophobic interactions between mAb-C molecules at high protein concentrations are probably not the only source that induce PPIs. Other weak intermolecular forces, such as dipole-dipole coupling, hydrogen bonding, or even electrostatic interactions, could also contribute to mAb-C RSA to some extent.[21]

Similar to the HX-MS analysis described in the companion paper with mAb-J,[4] potential chemical exchange rate differences in mAb-C formulated with the various additives prevent direct comparisons between HX kinetics in the different formulations.[36] Thus, we focused on HX difference between high and low protein concentrations of mAb-C in the presence of each additive separately. PPIs of mAb-C in BB were observed not only at the high concentration (60 mg/mL), but also, albeit to a much lower extent, at the low protein concentration (5 mg/mL). For example, this was seen by CG-MALS analysis examining the size distribution of mAb-C at ~1-20 mg/mL. HX-MS analysis was primarily based on the difference of RSA extent between high and low protein concentrations. Thus, we are comparing conditions with more versus less RSA, rather than complete versus no RSA. Such HX-MS analysis shows that several specific regions of mAb-C undergo PPI, resulting in protection of these regions from hydrogen exchange (Fig. 6a).

Effects of Hydrophobic (TMPAI and $TrpNH_2HCl$) and Chaotropic (GdnHCl) Salts on RSA of mAb-C

In the presence of the additives either with hydrophobic apolar character, including TMPAI (I^- is also a stronger chaotrope than Cl^-) and $TrpNH_2HCl$ (both at 0.15M), or with properties attributed to chaotropes, including GdnHCl (at 0.5M), HX-MS analysis shows several RSA regions within mAb-C had diminished protection from hydrogen exchange, especially at CDR H1, CDR H2, CDR L2, and CDR L3 (Figs. 6b-6d). Beyond the CDRs, there were a few additional regions of mAb-C that show protection at high concentration. For example, the end of C_H3 region in the presence of GdnHCl and both the beginning of C_H1 region and the end of C_H3 region in the presence of TMPAI and $TrpNH_2HCl$ manifest protection. Such phenomenon probably indicates that these 3 excipients could dissociate higher order oligomeric mAb-C complexes to smaller dimeric or trimeric forms (consistent with CG-MALS studies). Thus, the remaining interactions at C_H1 and C_H3 regions are possibly a signature of difference between dimeric and trimeric complexes of mAb-C.

Combining these HX-MS results with the biophysical and solution measurements, it can be seen that GdnHCl, TMPAI, and $TrpNH_2HCl$ all displayed an ability to disrupt RSA interactions within mAb-C with a rank ordering of effectiveness of GdnHCl > TMPAI > $TrpNH_2HCl$. Presumably, the major effects of these additives are mediated by the cations: $GdnH^+$, $TMPA^+$, and $TrpNH_3^+$. Several types of protein-excipient interactions (hydrogen bonding, preferential hydration, electrostatic interactions, dispersive interactions, cation$-\pi$ interactions) could each effectively disrupt the PPIs within proteins.[37,38] Although TMPAI and $TrpNH_2HCl$ have the potential for $\pi-\pi$ interactions (via their aromatic rings interacting with aromatic rings in amino acid residues in mAb-C), GdnHCl, as a chaotropic salt,[39] was more effective in terms of diminishing PPIs for mAb-C.[40] Preferential interactions of GdnHCl with mAb-C might more effectively compete PPIs.[38] However, comparisons are complicated because I^- from TMPAI is a stronger chaotrope than Cl^-.[41] Therefore, albeit similar properties exist between cations of TMPAI and $TrpNH_2HCl$, the anions of these 2 additives, including I^- and Cl^-, may play roles that differentiate their RSA-disrupting efficiency.[42,43] Furthermore, the size of the cations may also be a determining factor because their rank order by size is $GdnH^+$<$TMPA^+$<$TrpNH_2H^+$ which reverses the rank order of their effectiveness in disrupting RSA. Therefore, steric hindrance might decrease the tendency for larger excipients to interact with the surface of mAb-C; it may be easier for smaller excipients to access shallow pockets on the mAb-C surface. Consistent with this hypothesis, we found in protein-excipient docking analysis that there were more potential interaction sites for $GdnH^+$ than for the other 2 excipients (Fig. 7). Although GdnHCl showed greater ability to disrupt PPIs compared with the other 2 hydrophobic salts, the concentration used in this study was higher, and guanidine decreased the conformational stability of mAb-C, as indicated by lower thermal melting temperature values (data not shown).

Effects of Ethanol on RSA of mAb-C

In the case of the HX-MS results for mAb-C in the presence of 15% ethanol, several unique trends were observed. For example, many of the RSA regions within mAb-C were retained, except for the CDR L2 and CDR L3 regions, thus resulting in either a diminished RSA of mAb-C at 60 mg/mL or promotion of RSA at 5 mg/mL, but to a lesser extent than observed in the presence of either GdnHCl, TMPAI, and $TrpNH_2HCl$, or Na_2SO_4, respectively. In comparison to mAb-C in BB alone, there was also 1 region (middle of C_L1) that shows increased protection at high protein concentration in the presence of ethanol (Fig. 6e).

Ethanol, as a less polar solvent, was used to determine its effects on mAb-C PPIs. As shown in Figures 2, 3, 4, and 6, the results of relative solubility, DLS, CG-MALS, and HX-MS demonstrated a contradictory trends on the extent of RSA for mAb-C in the presence of ethanol. Moreover, the conformation of mAb-C was also easily perturbed as a function of temperature with ethanol in solution (data not shown). It has been broadly reported that ethanol could alter both intramolecular and intermolecular interactions by preferentially interacting with hydrophobic residues,[44-46] and it also, depending on the temperature, decreases protein solubility to different extents.[46-49] In fact, owing to lower protein solubility in ethanol,[50,51] the addition of ethanol led to the precipitation of mAb-C in high-concentration solutions during viscosity measurements, especially at lower temperatures. Finally, addition of ethanol could alter original solution hydrogen-bonding networks, surface tension, and density, which may further perturb the molecular behavior of mAb-C.[52,53] As a result, multiple effects of ethanol on mAb-C created diverse observations based on different biophysical or HX techniques, requiring more systemic studies to better understand its complicated effects on mAb-C.

Effects of Na_2SO_4 on RSA of mAb-C

In the presence of 0.15M Na_2SO_4, increased PPIs between mAb-C molecules were detected by HX-MS, showing overall an even more extensive extent of protection within the mAb-C RSA regions (Fig. 6f). Na_2SO_4 was the only additive examined in this work that promoted mAb-C RSA, as observed in all biophysical and HX-MS analyses. This resulted in a relatively higher dynamic viscosity as well as a larger hydrodynamic size (and a larger protein interaction parameter) of mAb-C complexes as measured by DLS. As a kosmotropic salt, Na_2SO_4 is excluded from surfaces of mAb-C molecules, and at the same time, it increases surface tension of bulk water, which likely contribute to mAb-C molecules forming relatively larger higher order oligomeric species (as shown in CG-MALS studies in Fig. 4).[54,55] In comparison to mAb-C in BB alone, 150 mM of Na_2SO_4 added to BB shows increased relative solubility of mAb-C, while 0.5 M of Na_2SO_4 reduced its solubility. At

relatively low concentrations (150 mM) of Na_2SO_4, salting-in (charge-shielding) effects are probably the dominant factor that increases mAb-C solubility as described by Debye-Hückel theory.[56] Essentially, mAb-C molecules are surrounded by salt counterions, screening their charges, which will decrease the electrostatic free energy of mAb-C molecules and increase solvent activity and finally lead to higher relative solubility.[56] At higher salt concentrations (0.5 M), however, salting-out effects begin to be dominant as the major influence. Here, water molecules are attracted by salt ions, and a decreased number of water molecules interact with mAb-C, leading to protein dehydration and thus stronger PPIs among mAb-C molecules and ultimately to protein precipitation.[57]

Conclusions

In this paper (Part 2) with mAb-C, along with a companion paper (Part 1) in this issue with mAb-J,[4] we examine the role of additives and excipients in disrupting and enhancing specific PPIs that lead to the RSA of 2 different IgG1 mAbs at high protein concentrations. In this work, the solution properties, molecular features, and backbone flexibility (at specific sites known to facilitate RSA) were evaluated for a human monoclonal IgG1 antibody (mAb-C), previously demonstrated to undergo RSA via Fab-Fab interactions (at specific peptide segments within the CDRs of mAb-C rich in hydrophobic amino acids). These parameters were evaluated in the presence a chaotropic salt (GdnHCl), hydrophobic salt (TMPAI), aromatic amino acid derivative ($TrpNH_2HCl$), kosmotropic salt (Na_2SO_4), and a less polar solvent (ethanol). The ability of these additives to disrupt RSA and improve the solution properties of mAb-C at high protein concentrations was demonstrated and rank ordered (GdnHCl > TMPAI > $TrpNH_2HCl$). Contradictory results were observed for ethanol probably because of the coexistence of multiple effects of the less polar solvent on mAb-C. Na_2SO_4, on the other hand, showed the opposite effect and promoted the RSA of mAb-C and resulted in less desirable solution properties.

In a companion paper (Part 1), similar experiments were performed with a different human IgG1 mAb (mAb-J) that displays RSA at high protein concentration primarily through a different molecular mechanism (charge interactions between Fab-Fc regions of the antibody).[14] A series of charged excipients were then employed in the companion paper to determine their effects on the solution properties, molecular attributes, and backbone flexibility. By examining 2 different human IgG1 mAbs (mAb-J and mAb-C) that undergo RSA by different molecular mechanisms, these 2 studies demonstrate a rational approach to the development of high-concentration mAb formulations by (1) determining the molecular mechanism of RSA by HX-MS analysis, (2) selecting specific additives expected to disrupt these known intermolecular interactions and rank order their ability to do so by HX-MS, and then (3) evaluating the effects of these specific additives on the solution properties (e.g., viscosity) and molecular attributes (e.g., size and relative solubility) of the mAb at high protein concentrations. This design approach for developing high-concentration mAb formulations with optimal solution properties would then be followed by a comparison of the real-time and accelerated storage stability of a mAb in the presence of the candidate additives for the final selection of the formulation composition.

Acknowledgments

This study was supported by a research grant from MedImmune LLC and an equipment loan from Agilent Technologies, Inc.

References

1. Armstrong NJ, Bowen MN, Maa Y-F. In: *High-Concentration Monoclonal Antibody Formulations*. Washington, DC: Google Patents, The Patent Cooperation Treaty (PCT); 2013. Available at: https://patents.google.com/patent/WO2013173687A1/en. Accessed July 2, 2019.
2. Shire SJ, Shahrokh Z, Liu J. Challenges in the development of high protein concentration formulations. *J Pharm Sci*. 2004;93(6):1390-1402.
3. Gibson TJ, McCarty K, McFadyen IJ, et al. Application of a high-throughput screening procedure with PEG-induced precipitation to compare relative protein solubility during formulation development with IgG1 monoclonal antibodies. *J Pharm Sci*. 2011;100(3):1009-1021.
4. Hu Y, Arora J, Joshi SB, et al. Characterization of excipient effects on reversible self-association, flexibility, and solution properties of an IgG1 monoclonal antibody at high concentrations: part 1 (Companion Manuscript). *J Pharm Sci*. 2019.
5. Liu J, Nguyen MDH, Andya JD, Shire SJ. Reversible self-association increases the viscosity of a concentrated monoclonal antibody in aqueous solution. *J Pharm Sci*. 2005;94(9):1928-1940.
6. Nishi H, Miyajima M, Nakagami H, Noda M, Uchiyama S, Fukui K. Phase separation of an IgG1 antibody solution under a low ionic strength condition. *Pharm Res*. 2010;27(7):1348-1360.
7. Mason BD, Zhang L, Remmele RL, Zhang J. Opalescence of an IgG2 monoclonal antibody solution as it relates to liquid−liquid phase separation. *J Pharm Sci*. 2011;100(11):4587-4596.
8. Connolly Brian D, Petry C, Yadav S, et al. Weak interactions govern the viscosity of concentrated antibody solutions: high-throughput analysis using the diffusion interaction parameter. *Biophys J*. 2012;103(1):69-78.
9. Lilyestrom WG, Yadav S, Shire SJ, Scherer TM. Monoclonal antibody self-association, cluster formation, and rheology at high concentrations. *J Phys Chem B*. 2013;117(21):6373-6384.
10. Raut AS, Kalonia DS. Liquid−Liquid phase separation in a dual variable domain immunoglobulin protein solution: effect of formulation factors and protein−protein interactions. *Mol Pharm*. 2015;12(9):3261-3271.
11. Raut AS, Kalonia DS. Opalescence in monoclonal antibody solutions and its correlation with intermolecular interactions in dilute and concentrated solutions. *J Pharm Sci*. 2015;104(4):1263-1274.
12. Baek Y, Zydney AL. Intermolecular interactions in highly concentrated formulations of recombinant therapeutic proteins. *Curr Opin Biotechnol*. 2018;53:59-64.
13. Saluja A, Badkar AV, Zeng DL, Nema S, Kalonia DS. Application of high-frequency rheology measurements for analyzing protein-protein interactions in high protein concentration solutions using a model monoclonal antibody (IgG2). *J Pharm Sci*. 2006;95(9):1967-1983.
14. Roberts CJ. Therapeutic protein aggregation: mechanisms, design, and control. *Trends Biotechnol*. 2014;32(7):372-380.
15. Barnett GV, Drenski M, Razinkov V, Reed WF, Roberts CJ. Identifying protein aggregation mechanisms and quantifying aggregation rates from combined monomer depletion and continuous scattering. *Anal Biochem*. 2016;511:80-91.
16. Geoghegan JC, Fleming R, Damschroder M, Bishop SM, Sathish HA, Esfandiary R. Mitigation of reversible self-association and viscosity in a human IgG1 monoclonal antibody by rational, structure-guided Fv engineering. *mAbs*. 2016;8(5):941-950.
17. Bethea D, Wu SJ, Luo J, et al. Mechanisms of self-association of a human monoclonal antibody CNTO607. *Protein Eng Des Sel*. 2012;25(10):531-537.
18. Teplyakov A, Obmolova G, Wu SJ, et al. Epitope mapping of anti-interleukin-13 neutralizing antibody CNTO607. *J Mol Biol*. 2009;389(1):115-123.
19. Nishi H, Miyajima M, Wakiyama N, et al. Fc domain mediated self-association of an IgG1 monoclonal antibody under a low ionic strength condition. *J Biosci Bioeng*. 2011;112(4):326-332.
20. Yadav S, Laue TM, Kalonia DS, Singh SN, Shire SJ. The influence of charge distribution on self-association and viscosity behavior of monoclonal antibody solutions. *Mol Pharm*. 2012;9(4):791-802.
21. Arora J, Hickey JM, Majumdar R, et al. Hydrogen exchange mass spectrometry reveals protein interfaces and distant dynamic coupling effects during the reversible self-association of an IgG1 monoclonal antibody. *mAbs*. 2015;7(3):525-539.
22. Esfandiary R, Parupudi A, Casas-Finet J, Gadre D, Sathish H. Mechanism of reversible self-association of a monoclonal antibody: role of electrostatic and hydrophobic interactions. *J Pharm Sci*. 2015;104(2):577-586.
23. Arora J, Hu Y, Esfandiary R, et al. Charge-mediated Fab-Fc interactions in an IgG1 antibody induce reversible self-association, cluster formation, and elevated viscosity. *mAbs*. 2016;8(8):1561-1574.
24. Middaugh CR, Tisel WA, Haire RN, Rosenberg A. Determination of the apparent thermodynamic activities of saturated protein solutions. *J Pharm Sci*. 1979;254:367-370.
25. Arora J, Hu Y, Esfandiary R, et al. Charge-mediated Fab-Fc interactions in an IgG1 antibody induce reversible self-association, cluster formation, and elevated viscosity. *mAbs*. 2016;8:1561-1574. Manuscript submitted.
26. Padlan EA. Anatomy of the antibody molecule. *Mol Immunol*. 1994;31(3):169-217.
27. Matsumiya S, Yamaguchi Y, Saito J, et al. Structural comparison of fucosylated and nonfucosylated Fc fragments of human immunoglobulin G1. *J Mol Biol*. 2007;368(3):767-779.

28. *Molecular Operating Environment (MOE), 2013.08*. Montreal, QC, Canada: Chemical Computing Group ULC; 2018.
29. Kalonia C, Toprani V, Toth R, et al. Effects of protein conformation, apparent solubility, and protein–protein interactions on the rates and mechanisms of aggregation for an IgG1Monoclonal antibody. *J Phys Chem B*. 2016;120(29):7062-7075.
30. Reth M. Matching cellular dimensions with molecular sizes. *Nat Immunol*. 2013;14(8):765-767.
31. Chow C-K, Allan BW, Chai Q, Atwell S, Lu J. Therapeutic antibody engineering to improve viscosity and phase separation guided by crystal structure. *Mol Pharm*. 2016;13(3):915-923.
32. Wu SJ, Luo J, O'Neil KT, et al. Structure-based engineering of a monoclonal antibody for improved solubility. *Protein Eng Des Sel*. 2010;23(8):643-651.
33. Whitaker N, Xiong J, Pace SE, et al. A formulation development approach to identify and select stable ultra–high-concentration monoclonal antibody formulations with reduced viscosities. *J Pharm Sci*. 2017;106(11):3230-3241.
34. Easterbrook-Smith SB, Vandenberg RJ, Alden JR. The role of Fc: Fc interactions in insoluble immune complex formation and complement activation. *Mol Immunol*. 1988;25(12):1331-1337.
35. Carpenter JF, Crowe JH. The mechanism of cryoprotection of proteins by solutes. *Cryobiology*. 1988;25(3):244-255.
36. Toth RT, Mills BJ, Joshi SB, et al. Empirical correction for differences in chemical exchange rates in hydrogen exchange-mass spectrometry measurements. *Anal Chem*. 2017;89(17):8931-8941.
37. Kamerzell TJ, Esfandiary R, Joshi SB, Middaugh CR, Volkin DB. Protein–excipient interactions: mechanisms and biophysical characterization applied to protein formulation development. *Adv Drug Deliv Rev*. 2011;63(13):1118-1159.
38. Hong T, Iwashita K, Shiraki K. Viscosity control of protein solution by small solutes: a review. *Curr Protein Pept Sci*. 2018;19(8):746-758.
39. Zangi R. Can salting-in/salting-out ions be classified as chaotropes/kosmotropes? *J Phys Chem B*. 2009;114(1):643-650.
40. Oki S, Nishinami S, Shiraki K. Arginine suppresses opalescence and liquid–liquid phase separation in IgG solutions. *Int J Biol Macromol*. 2018;118:1708-1712.
41. Zhang Y, Cremer PS. Interactions between macromolecules and ions: the Hofmeister series. *Curr Opin Chem Biol*. 2006;10(6):658-663.
42. Ahmed M, Namboodiri V, Singh AK, Mondal JA. On the intermolecular vibrational coupling, hydrogen bonding, and librational freedom of water in the hydration shell of mono-and bivalent anions. *J Chem Phys*. 2014;141(16):164708.
43. Dougherty RC. Density of salt solutions: effect of ions on the apparent density of water. *J Phys Chem B*. 2001;105(19):4514-4519.
44. Brandts JF, Hunt L. Thermodynamics of protein denaturation. III. Denaturation of ribonuclease in water and in aqueous urea and aqueous ethanol mixtures. *J Am Chem Soc*. 1967;89(19):4826-4838.
45. Brandts JF. The thermodynamics of protein denaturation. I. The denaturation of chymotrypsinogen. *J Am Chem Soc*. 1964;86(20):4291-4301.
46. Yoshizawa S, Arakawa T, Shiraki K. Dependence of ethanol effects on protein charges. *Int J Biol Macromol*. 2014;68:169-172.
47. Pace CN, Trevino S, Prabhakaran E, Scholtz JM. Protein structure, stability and solubility in water and other solvents. *Philos Trans R Soc Lond B Biol Sci*. 2004;359(1448):1225-1235.
48. Yoshikawa H, Hirano A, Arakawa T, Shiraki K. Effects of alcohol on the solubility and structure of native and disulfide-modified bovine serum albumin. *Int J Biol Macromol*. 2012;50(5):1286-1291.
49. Yoshikawa H, Hirano A, Arakawa T, Shiraki K. Mechanistic insights into protein precipitation by alcohol. *Int J Biol Macromol*. 2012;50(3):865-871.
50. Chin JT, Wheeler SL, Klibanov AM. On protein solubility in organic solvent. *Biotechnol Bioeng*. 1994;44(1):140-145.
51. Tscheliessnig A, Satzer P, Hammerschmidt N, Schulz H, Helk B, Jungbauer A. Ethanol precipitation for purification of recombinant antibodies. *J Biotechnol*. 2014;188:17-28.
52. Ghoufi A, Artzner F, Malfreyt P. Physical properties and hydrogen-bonding network of water–ethanol mixtures from molecular dynamics simulations. *J Phys Chem B*. 2016;120(4):793-802.
53. Li F, Men Z, Li S, Wang S, Li Z, Sun C. Study of hydrogen bonding in ethanol-water binary solutions by Raman spectroscopy. *Spectrochim Acta A Mol Biomol Spectrosc*. 2018;189:621-624.
54. Curtis RA, Prausnitz JM, Blanch HW. Protein protein and protein salt interactions in aqueous protein solutions containing concentrated electrolytes. *Biotechnol Bioeng*. 1998;57(1):11-21.
55. Wayne Melander CH. Salt effects on hydrophobic interactions in precipitation and chromatography of proteins: an interpretation of the lyotropic series. *Arch Biochem Biophys*. 1977;183(1):200-215.
56. Long FA, McDevit WF. Activity coefficients of nonelectrolyte solutes in aqueous salt solutions. *Chem Rev*. 1952;51(1):119-169.
57. Duong-Ly KC, Gabelli SB. Salting out of proteins using ammonium sulfate precipitation. *Methods Enzymol*. 2014;541:85-94.